

# UC Riverside

## UC Riverside Previously Published Works

### Title

Firsthand cigarette smoke alters fibroblast migration and survival: implications for impaired healing

### Permalink

<https://escholarship.org/uc/item/1wp204tf>

### Journal

Wound Repair and Regeneration, 12(4)

### ISSN

1067-1927

### Authors

Wong, L S  
Martins-Green, Manuela

### Publication Date

2004-07-01

Peer reviewed

---

# Firsthand cigarette smoke alters fibroblast migration and survival: implications for impaired healing

LINA S. WONG, BS<sup>a,b</sup>; MANUELA MARTINS-GREEN, PhD<sup>a</sup>

---

Although it is known that high levels of cigarette smoke lead to cell death, little is known about the effects of low-to-moderate levels of smoke components that are found in vivo, such as those experienced by cells in tissues. Clinical studies and experimental data show that smokers heal poorly and are more prone to develop fibrotic diseases. Here we show the effects of first-hand cigarette smoke on fibroblasts, cells that are critically involved in these processes. Using doses of smoke found in the tissues of smokers and a variety of cell and molecular approaches, we show that these doses of cigarette smoke do not cause cell death but rather stimulate fibroblasts to produce stress response and survival proteins such as interleukin-8, PKB/Akt, p53, and p21 that in turn contribute to an increase in cell survival. In addition, smoke-treated cells show a decrease in cell migration, which can be explained by the increased cell adhesion and alterations in cytoskeletal elements. We also show that these levels of smoke cause changes in mitochondrial morphology with a minimum loss of function and these changes are the result of exposure to reactive oxygen species. We conclude that the increase in cell survival may lead to a build-up of connective tissue in the area of a wound, potentially leading to delayed healing and/or fibrosis and that the alterations in the cytoskeleton and in cell adhesion result in inhibition of cell migration, a process that could lead to nonclosure of the wound for lack of proper fibroblast migration to form the healing tissue. (**WOUND REP REG 2004;12:471-484**)

---

It has been clinically and experimentally shown that cigarette smokers suffer from impaired wound healing,<sup>1-5</sup> an important medical concern, especially for surgeons, because patients who smoke are at increased risk of complications and a decrease in the quality of postoperative results.<sup>6-8</sup> Fibroblasts are critical cells involved in the process of repair and are exposed and affected by smoke components circulating in the blood stream.<sup>9</sup> This effect is quite evident, for example, in the skin of the face of women who have smoked for many years. The skin loses elasticity, a process that is intim-

*From the Department of Cell Biology and Neuroscience<sup>a</sup> and the Graduate Group of Biomedical Sciences<sup>b</sup>, University of California, Riverside, California.*

*Manuscript received: October 27, 2003*

*Accepted in final form: March 4, 2004*

*Reprint requests: Professor Manuela Martins-Green, Department of Cell Biology and Neuroscience, University of California Riverside, Riverside, CA 92521. Fax: (909) 787-4286; Email: mmgreen@ucr.ac1.ucr.edu.*

*Copyright © 2004 by the Wound Healing Society.*

*ISSN: 1067-1927 \$15.00 + 0.*

BrdU	Bromodeoxyuridine
BSA	Bovine serum albumin
CAT	Catalase
CEF	Chicken embryonic fibroblast
ECM	Extracellular matrix
GAPDH	Glyceraldehyde 3-phosphate dehydrogenase
IL-8	Interleukin-8
MSW	Mainstream-whole
PBS	Phosphate buffered saline solution
RNS	Reactive nitrogen species
ROS	Reactive oxygen species
SOD	Superoxide dismutase
SSW	Sidestream-whole
TTBS	Tween-tris buffered saline solution

ately linked to abnormalities in the dermis that in turn are linked to dermal fibroblast function.<sup>10,11</sup> In addition, it is well known that when surgeons need to perform surgery on people who smoke, they require that the person stop smoking for a period of time before the operation.<sup>6,12</sup> This is not only to improve lung function, but also to avoid problems with healing. Furthermore, open wounds, for example in diabetic

people, have exposed connective tissue and sometimes fascia that absorb smoke components from the environment, affecting the development of the healing tissue.<sup>13</sup> This problem is compounded by the absorption of cigarette smoke components by the dressings, much like the absorption by drapes, wallpaper, clothing, and upholstery of furniture.

It is now clear that the effects of cigarette smoke are not limited to cosmetic problems but that the cosmetic response reflects an underlying systemic problem introduced by smoking. In some cases smokers heal poorly<sup>14</sup> and in other cases they over-heal.<sup>15</sup> Despite the many clinical implications pointing to the detrimental effects of tobacco use on wound healing, very little is known about the effects of cigarette smoke on the function of cells that are critical for proper healing, e.g., fibroblasts.

During wound healing, fibroblasts are critically involved in producing cytokines involved in the inflammatory response, and they are key players during the formation of the healing (granulation) tissue. Upon injury, fibroblasts respond by first secreting a variety of cytokines, in particular, chemokines. The latter proteins attract leukocytes that during the inflammatory phase fight off infection and initiate the healing response. In the subsequent phase of wound healing, fibroblasts are involved in granulation tissue formation by proliferating, migrating, depositing, and remodeling the extracellular matrix (ECM) through new synthesis and remodeling of the matrix molecules. In addition, fibroblasts differentiate into myofibroblasts, cells that are instrumental in wound closure and contraction.<sup>16</sup> Development of the fibroblast-rich granulation tissue during wound healing is tightly controlled and is critical for the formation of a healthy scar. Deregulation of this process result in many severe consequences, including impaired healing and/or fibrotic diseases.<sup>16,17</sup> Because fibroblasts are "orchestrators" of the healing process, studying the effects of cigarette smoke on the structure and function of these cells will provide insight into specific mechanisms involved in impaired wound healing in smokers, and potentially could lead to prevention of postoperative wound healing complications.

There are generally two types of smoke: mainstream smoke ("first-hand") is the smoke inhaled by the smoker, and sidestream smoke (a main component of environmental tobacco smoke), is the smoke given off from the burning end of the cigarette during intervals between puffs. Both smokes are a complex mixture of particulate matter, volatile acids, and gases. "First-hand" smoke is rich in reactive oxygen species (ROS) and reactive nitrogen species (RNS).<sup>18</sup> It has been shown that an imbalance between the production of antioxidants in cells and exposure to excessive amounts of ROS and RNS can lead to a state of "oxidative stress" that can lead to cell death.<sup>19</sup> However, the

outcome is unknown when cells are exposed to levels of cigarette smoke found in tissues of smokers, hence the studies presented here focus on the effects of these levels of smoke on fibroblast structure and function. In addition, unlike the majority of smoke studies, which mostly focus on specific components of cigarette smoke or smoke extracts, we studied the effects of complex mixtures of whole cigarette smoke.

We show for the first time that nonlethal levels of mainstream-whole (MSW) smoke stimulate cellular stress responses that contribute to cell survival rather than cell death. In addition, these levels of smoke lead to inhibition of fibroblast migration, a process that is critical for proper healing. In combination, these two effects could be responsible for many of the healing problems encountered by smokers.

## MATERIALS AND METHODS

Mainstream-whole (MSW) and sidestream-whole (SSW) smoke solutions were prepared in serum free Medium 199 (Gibco-BRL, Grand Island, NY) using 2R1 research-grade cigarettes (University of Kentucky, Louisville, KY). The puffs of smoke were drawn through 199 serum-free medium using a puffer box built by the University of Kentucky. These puffs are equivalent to those inhaled by an active smoker.<sup>20</sup> The pH of each solution was adjusted to 7.4 before adding to primary fibroblasts.

### Smoke quantitation by gas chromatography

To quantify the smoke solution, we used nicotine as a marker. To extract the nicotine, 300  $\mu$ l of smoke solution was mixed with 6  $\mu$ l of 1 M NaOH to raise the pH to  $\sim$ 10, thus deprotonating the nicotine and enabling its partition into a nonpolar organic solvent. To this solution, 1 ml of pentane containing 4  $\mu$ g/ml of 2-benzylamino/ml of 2-benzylaminopyridine (internal standard) was added and mixed by shaking for  $\sim$ 1 minute to allow the nicotine to partition into the organic phase. The organic phase was removed and the aqueous phase extracted again with 1 ml of pure pentane (without internal standard). The two organic extracts were combined, evaporated to dryness under a stream of dry nitrogen gas, and re-dissolved in 100  $\mu$ l of dichloromethane. A 1  $\mu$ l aliquot of this solution was injected into a fused-silica DB-1 column (J & W Scientific, Folsom, CA). The injection port temperature was 250  $^{\circ}$ C, the carrier gas (helium) flow rate was 1 ml/minute, and the initial column temperature was 40  $^{\circ}$ C. After 1 minute, the temperature was increased at 40  $^{\circ}$ C/minute to 170  $^{\circ}$ C and then at 2  $^{\circ}$ C/minute to 190  $^{\circ}$ C. The column was then cleared of residuals by increasing the temperature at 40  $^{\circ}$ C/minute to 250  $^{\circ}$ C, where it was held for 15 minutes. Compounds eluting from the column were monitored by flame ionization detection, and the signal was

processed through an integrator. Nicotine content was determined by calculating the ratio between the peak area for nicotine and the 2-benzylaminopyridine internal standard, and comparing to a standard curve prepared with known amounts of nicotine. The correlation coefficient of the standard curve was 0.9995. The amount of nicotine in MSW is  $\sim 5.17$   $\mu\text{g/ml/cigarette}$ .

### **Cell culture**

Primary cultures of chicken embryo fibroblasts (CEFs) were prepared from 10-day-old chicken embryos as described previously.<sup>21</sup> On the fourth day, secondary cultures were prepared by trypsinizing and plating the primary cells in Medium 199 containing 0.3 percent tryptose phosphate broth and 2 percent donor calf serum at a density of  $0.3 \times 10^6$  cells/35 mm plate for 3 days to reach confluency. To study the effects of MSW or SSW smoke on CEFs or normal human dermal fibroblasts, these were exposed to the smoke solutions at 37 °C, 5 percent CO<sub>2</sub> for varying periods of time.

### **Flow cytometry**

Fibroblasts were plated at  $1.2 \times 10^6$  cells/60 mm plate, allowed to grow to confluency and treated with MSW or SSW for 4 hours. Cells were then trypsinized (500  $\mu\text{l}$ ), centrifuged at 3500 r.p.m. for 5 minutes and stained with 50 nM DiOC6 (Molecular Probes, Inc., Eugene, OR) in warm phosphate buffered saline solution (PBS) for 10 minutes, rinsed once with warm PBS, and resuspended in 200  $\mu\text{l}$  of PBS. PBS was warmed in a 37 °C water bath. Cells were then loaded into a FACScan machine (Becton Dickinson Immunocytometry Systems, San Jose, CA). Excitation was at 488 nm and emission detected at 530 nm.

### **ATP assay**

The CellTiter-Glo Luminescent Cell Viability Assay kit (Promega, Inc., Madison, WI) was used following the manufacturer's instruction with a small modification as briefly detailed below. Cells were plated at  $3 \times 10^4$  cells/well in a 96-well plate (Costar, Inc., Acton, MA). After confluency, cells were treated with MSW for 18 hours, and 30 minutes before the end of the treatment the cells were removed from the 37 °C incubator and placed at room temperature for equilibration. The substrate was then added, incubated for 10 minutes to lyse the cells, the reaction mixed, transferred to a white nontransparent 96-well plate (Costar, Inc.), and read in a BMG LUMIstar Galaxy Luminometer (Durham, NC) with a 1-second integration time, 120-second cycle time and a 75 gain. Experiments were done in triplicates and repeated at least three times.

### **Fluorescence labeling**

Labeling with MitoTracker Red (Molecular Probes, Inc.) was performed according to the manufacturer's

protocol. Briefly, fibroblasts were treated with MSW for 4 hours and stained with (50 nM) Mitotracker Red (CMXRos) for 10 minutes in warm media, then fixed for 15 minutes in 4 percent paraformaldehyde and mounted with VectaShield (Vector Laboratories, Burlingame, CA). Fluorescence pictures were taken with a Zeiss LSM510 confocal microscope. For rhodamine phalloidin labeling, cells were plated at  $0.3 \times 10^6$  cells per 35 mm plate. After 4 hours of treatment with MSW, cells were washed with PBS and fixed in 4 percent paraformaldehyde for 30 minutes at room temperature. At the end of this period, cells were washed three times with PBS and 0.1 percent Triton-X-100 was added and allowed to incubate for 10 minutes. Cells were then washed three times with PBS and rhodamine phalloidin (5 units/ml or 0.165  $\mu\text{M}$ ) was added and allowed to incubate at room temperature for 20 minutes. The stained cells were then washed three times and mounted with VectaShield and sealed with nail polish. Pictures were taken with a MicroPhot FXA fluorescence microscope (Nikon, Garden City, NY). For quantification of the F-actin, the procedure was similar to that described above except that the cells were treated with 0.2 percent Triton-X-100 for 10 minutes after fixation and 0.1 M NaOH was added to extract the cells after rhodamine phalloidin staining. The level of fluorescence was measured with a fluorimeter at 550–580 nm.

### **Immunolabeling of proteins**

Vinculin and microtubules were detected as follows. Plates of fibroblasts were treated with MSW as described above. After 4 hours, the cells were rinsed with PBS, fixed in 4 percent paraformaldehyde, permeabilized with 0.1 percent Triton X-100, and incubated with PBS containing 0.1 M glycine for 10 minutes. Cells were blocked for 30 minutes with 10 percent goat or sheep serum in PBS, incubated with mouse anti-vinculin (1:50; Hybridoma Bank, University of Iowa, Iowa City, IA) or mouse anti-tubulin (1:200; Sigma-Aldrich, St. Louis, MO) in 1 percent bovine serum albumin (BSA)/PBS for 1 hour at room temperature, and washed three times with 0.1 percent BSA/PBS for 10 minutes each. The cells were then incubated in goat anti-mouse FITC or sheep anti-mouse Texas Red (1:100) in 1 percent BSA/PBS for 1 hour at room temperature, washed three times for 10 minutes with 0.1 percent BSA in PBS, and mounted with Vectashield. Confocal fluorescence microscopy was performed on a ZEISS LSM510.

### **Preparation of cytoplasmic extracts and immunoblot analysis for cytochrome C analysis**

To obtain cytoplasmic extracts, cells were plated in 35 mm dishes as described above. After treatment, cells were rinsed in Tris-Glucose and 100–150  $\mu\text{l}$  of

0.05 percent Triton-X-100 was added, incubated at room temperature for 1–2 minutes before collecting the cytosolic extract. Cell lysates were then collected with 100  $\mu$ l 150 mM RIPA buffer in the presence of protease inhibitors.

### **Immunoblot analysis**

To detect the stress response protein interleukin-8 (IL-8), cell culture supernatants were collected in the presence of protease inhibitors. Equal volumes of the cell culture supernatants corresponding to equal protein concentration in the cell extracts were loaded on 20 percent polyacrylamide-glycerol gels and electrophoresed at 16–32 mA for about 3 hours. Transfer was performed in a semidry transfer apparatus (Millipore), and the chemokine IL-8 was immunolabeled using polyclonal antibodies as previously described (rabbit serum was prepared by Robert Sargeant [Ramona, CA]).<sup>22</sup> For detection of p21, PKB/Akt, and p53, cells were treated as above, cell lysates were extracted using 150 mM RIPA in the presence of protease inhibitors and equal concentration of protein (determined by the DC protein assay kit from Bio-Rad Laboratories, Hercules, CA) was loaded into a 7.5 percent or 10 percent Doucet gel.<sup>23,24</sup> The gel was then transferred to a nitrocellulose membrane using wet-transfer apparatus (Bio-Rad) at 100 V for 1 hour. The membranes were blocked for 1 hour in 5 percent milk in Tween-Tris buffered saline solution (TTBS) and then incubated overnight at 4 °C in primary antibodies to cytochrome C (1:500), p21 (1:400; Santa Cruz Biotechnology, Inc., Santa Cruz, CA), PKB/Akt (2  $\mu$ g/ml; Upstate Biotechnology, Lake Placid, NY); PKB/Akt-p (ser-473 1:1000; Cell Signaling Technology, Inc., Beverly, MA), p53 (1:1000; Oncogene Research Products, Inc., San Diego, CA), vinculin (1:200), or microtubules (1:200) in 1 percent milk in TTBS. The membranes were washed three times for 10 minutes each with TTBS, incubated in anti-mouse or anti-rabbit HRP (1:10,000; Amersham Pharmacia, Inc., Piscataway, NJ) in 1 percent milk for 1 hour and washed as above, and the bands were visualized using enhanced chemiluminescent (ECL; Amersham Pharmacia). All blots were reprobated for glyceraldehyde-3-phosphate dehydrogenase (GAPDH) to ensure that the samples were equally loaded.

### **Proliferation assays using 5-bromo-deoxyuridine**

5-Bromo-deoxyuridine (BrdU) incorporation assay was performed according to manufacturer's instructions (Oncogene Research Products). Cells were plated in 96-well plates and allowed to be confluent. BrdU was added along with the MSW treatment for specific time points. The cells were fixed, denatured, and incubated for 30 minutes at room temperature. The samples were then incubated with anti-BrdU antibody for 1 hour at

room temperature and washed three times. Goat anti-mouse IgG HRP conjugate (Amersham Pharmacia) was added for 30 minutes followed by substrate addition and incubation in the dark for 15 minutes. At this time, the reactions were stopped and the samples read at a dual wavelength of 450–570 nm.

### **Recovery experiment using flow cytometry**

Cells were plated at  $0.3 \times 10^6$  cells/35 mm plate in Medium 199 as described above and cultured to reach confluency. They were treated with MSW solution in serum-free media for 18 hours. At the end of the treatment, fresh medium was added and cells were allowed to recover for 24 hours. At the end of this period, the cells were photographed and treated again for 18 hours, then typsinized, resuspended in Isoton solution (Beckman Coulter, Inc., Fullerton, CA), and counted in a Coulter counter (Model Z2; Beckman Coulter). Another batch of cells was allowed to recover for another time and treated again before the cell number was measured.

### **Lysate for PKB detection**

For PKB/Akt detection, cells were extracted according to manufacturer's protocol (New England Biolabs, Inc., Beverly, MA). Briefly, cells were plated at  $2 \times 10^6$  cells/35 mm plate and cultured in medium containing no fetal calf serum overnight to reduce basal levels of phosphorylation. The following day, the medium was aspirated, fresh serum free media added, and the cells were allowed to incubate for 2 hours. Cells were treated with MSW in the presence of fresh serum-free media for the pertinent times. Cells were washed with 1 $\times$  PBS, lysed in 1 $\times$  sodium dodecyl sulfate sample buffer (100  $\mu$ l/35 mm plate or 500  $\mu$ l/plate of 100 mm plate), immediately scraped, and the extract transferred to a microcentrifuge tube and kept on ice. The samples were sonicated for 10–15 seconds to shear DNA and reduce sample viscosity. The samples were heated to 95–100 °C for 5 minutes, cooled on ice, microcentrifuged for 5 minutes, and equal amounts of protein loaded onto 10 percent sodium dodecyl sulfate-polyacrylamide electrophoresis gel.

### **Cloning ring migration assay**

Fibroblasts were plated at  $0.3 \times 10^6$  cells in a cloning ring. Cells were allowed to adhere for 3 hours. The edge of the ring formed by the cells were marked and then treated with MSW and allowed to migrate for 24 hours. At the end of the treatment time, migration distance was measured using a micrometer measuring from the edge of the initial ring to where the cells had migrated.

### **Statistical analysis**

All data were expressed as mean  $\pm$  SEM. Significance was determined using Student's *t*-test for comparison

between two means. Means were considered significantly different when  $p \leq 0.05$ .

## RESULTS

We have used primary CEFs and a variety of cellular and molecular approaches to study the effects of a complex mixture of “first-hand” or MSW smoke components on these cells. We used embryonic fibroblasts because it has been known for many years that these cells behave very much like wound fibroblasts.<sup>25</sup>

We quantified the smoke solution to ensure that the same dose of smoke components was consistently delivered to the cells and that the dilutions used to treat the cells were within the range of toxicants found in tissues. Nicotine was used as a marker to measure the concentration of our smoke solution because it is a commonly used biomarker in smoking-related studies<sup>20,26,27</sup> and it can be effectively measured by gas chromatography in our smoke solutions. The average serum level of nicotine in human smokers is 0.04  $\mu\text{g/ml}$  or as high as 0.072  $\mu\text{g/ml}$  in more chronic smokers.<sup>20,28–31</sup> It has been determined that the concentration of nicotine found in the organs is 15–25 times higher than that found in the blood of smokers,<sup>32–35</sup> hence 0.6–1  $\mu\text{g/ml}$  of tissue volume.

Fibroblasts were first treated with a range of MSW smoke solutions diluted from 1:2, 1:4, and 1:9 (smoke to media), whereas controls were incubated under the same conditions but without addition of smoke solutions (Figure 1). We found that 18 hours after treatment with a 1:9 dilution the cells were somewhat more elongated than the control (Figure 1B), but treatment with double this concentration (1:4 dilution) resulted in accentuated cell elongation and separation of cells from each other (Figure 1C). However, the cells recovered well after 24 hours in fresh medium, returning to the morphology of the control cells (Figure 1E). Solutions more concentrated than 1:4 resulted in considerable cell death (Figure 1D). Because we were interested in determining the effects of nonlethal doses of smoke on cell function, we used concentrations of smoke solution that affected the cells but did not cause cell death (i.e., 1:4 and lower). The 1:9 and 1:4 dilutions correspond to nicotine concentrations of  $\sim 0.5$  and 1.03  $\mu\text{g/ml}$ , respectively. Therefore, the MSW smoke solutions we used are well within the range of that found in human tissues.

To confirm that the cells treated with 1:4 dilutions of MSW were healthy and not undergoing apoptosis, we analyzed the cells by fluorescence-activated cell sorting. The majority of the cells in the untreated and MSW-treated groups showed high forward scattering properties, suggesting a smooth cell surface which is indicative of healthy cells (Figure 2A and B). In contrast, many cells treated with staurosporine

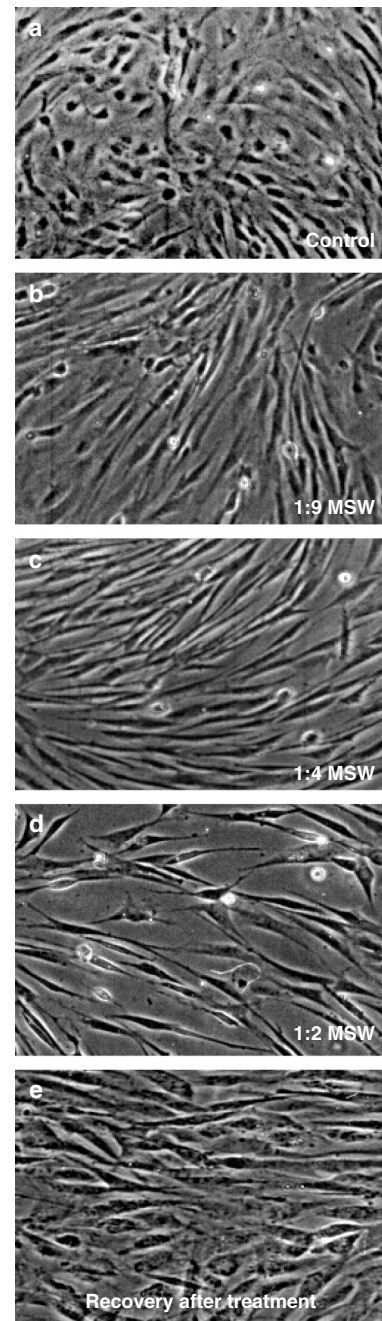


**FIGURE 1.** Phase-contrast microscopy of primary fibroblasts treated with MSW smoke solutions. Cells were treated with different doses of MSW in serum-free medium for 18 hours. Control cells were treated identically except that no smoke solution was added to the medium. (A) Untreated cells. (B) Cells treated with 1:9 MSW : medium ( $\sim 0.5$   $\mu\text{g/ml}$  of nicotine) began to show an elongated morphology. (C) Cells treated with 1:4 MSW : medium ( $\sim 1.03$   $\mu\text{g/ml}$  of nicotine) show a more pronounced effect on cell elongation and noticeable cell separation. (D) Cells treated with 1:2 MSW : medium ( $\sim 2.06$   $\mu\text{g/ml}$  of nicotine) became much more elongated but at the same time there was significant cell death. Pictures are representative of at least three experiments performed with different batches of primary cells. (E) Cells recovered after treatment with smoke solution (1:4). The morphology of the cells is healthy after being recovered for 24 hours in fresh medium.

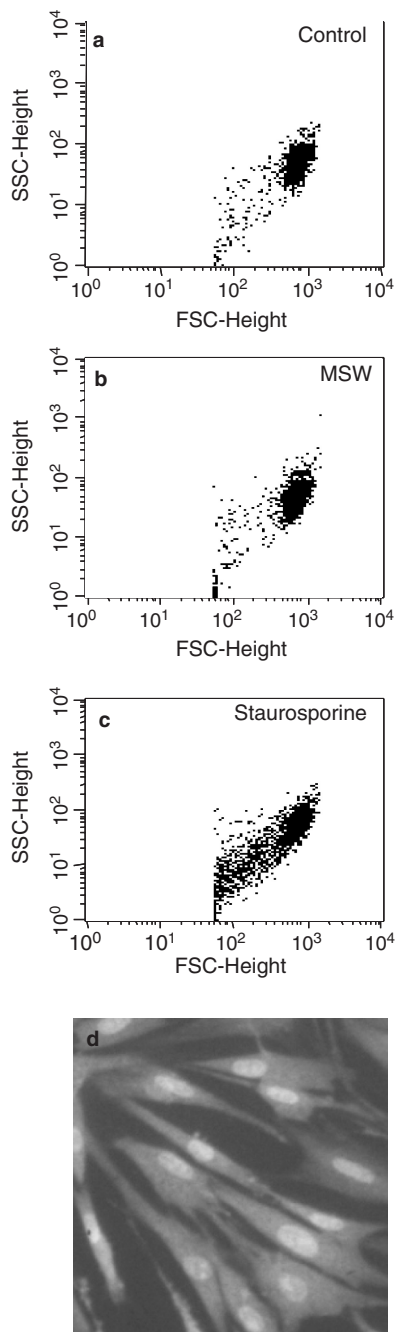


**FIGURE 2.** Fluorescence-activated cell sorter analysis of cells treated with MSW smoke. (A–C) Cells were treated with 1 : 4 MSW or with staurosporine. MSW-treated or untreated cells showed significantly fewer side scattering properties than staurosporine-treated cells (positive control), indicating that the smoke is not causing cell death and that the overall structure of the cell is normal. Each graph represents 10,000 events. (D) Cells stained with ethidium bromide and acridine orange after treatment with MSW showed normal cell morphology; no membrane blebbing was detected. Pictures are representative of at least three experiments performed with different batches of primary cells. SSC = side-scatter; FSC = forward-scatter.

(positive control), a molecule known to induce cell death, showed lower forward scattering properties, suggesting more cell surface irregularities and smaller particles reflecting cell breakdown (Figure 2C). Staurosporine caused an average of 40.8 percent cell death out of 10,000 events, whereas in the same number of events, untreated and MSW-treated cells exhibited only 9.5 percent and 9.7 percent cell death, respectively.

In addition, we stained cells with acridine/ethidium bromide to ascertain the state of the nucleus and the plasma membrane; neither showed blebbing, a feature that develops during apoptosis (Figure 2D). This was further confirmed by DNA laddering, another assay used to determine whether cells are dying; MSW did not induce breakdown of the chromatin (data not shown).

### ***Effects of MSW on mitochondrial structure and function***

Although doses of smoke components found in tissues of smokers do not appear to cause cell death, this type of smoke is rich in ROS and excess ROS can interfere with mitochondrial function, which is critical for normal cell physiology. Therefore, we examined the effects of MSW on the structure and function of the mitochondria. We visualized integrity of the structural mitochondria by staining treated and control cells with the fluorescent dye, Mitotracker Red, a cationic dye that enters the mitochondria and remains inside if the membrane potential is intact. Control cells showed long sausage-like mitochondria in an intertwined pattern that extended throughout the cytosol, and the dye was retained inside the mitochondria (Figure 3A). In the cells treated with MSW the mitochondria changed morphology and became more vesicle-like but they still retained the dye inside, suggesting that the membrane potential remains intact (Figure 3B). These effects were specific for MSW; the mitochondria in cells treated with SSW smoke (which is poor in ROS) were very similar to those of the control cells (data not shown). To confirm that the membrane potential of the mitochondria was not significantly affected, we performed flow cytometry analysis using DIOC6, a cell-permeable fluorescent dye that is frequently used for these assays. The DIOC6 dye will remain inside healthy mitochondria and is highly fluorescent if the membrane potential is undisturbed. However, in cells with altered mitochondrial membrane potential, the dye will diffuse out, leading to a decrease in intensity of fluorescence. We observed that in MSW-treated cells, the intensity of the dye was as strong as in control cells or SSW-treated cells, suggesting that the MSW effects on mitochondria do not disturb the membrane potential (Figure 3C). Staurosporine was used as a positive control because it has been shown that this molecule disrupts the

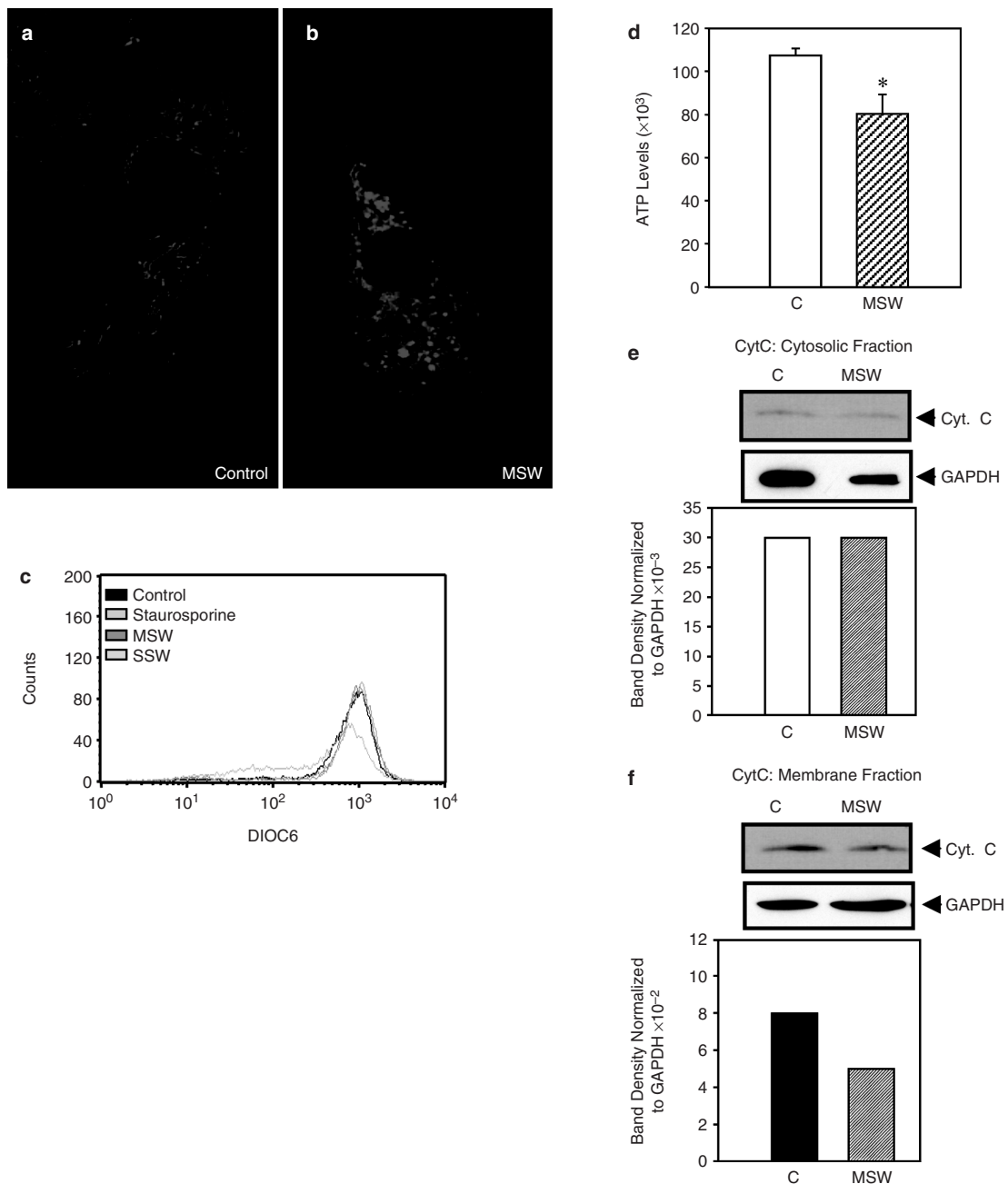


**FIGURE 3.** MSW does not significantly affect mitochondrial function. (A and B) Fibroblasts treated with 1 : 4 MSW smoke solution were stained with Mitotracker Red, which specifically stains normal functioning mitochondria, and analyzed by confocal microscopy. Control cells showed a long interconnected network of mitochondria extending throughout the cytoplasm (A); MSW- treated cells showed globular staining, indicating fragmentation of the mitochondrial network (B). (C) Fluorescence-activated cell sorter analysis using DIOC6 to test for intact membrane potential. Overlay of a representative histogram from each sample group indicates a shift of fluorescent intensity to the left in staurosporine-treated cells (positive control). This was not observed in the untreated samples or in the MSW-treated samples. Therefore, cigarette smoke appears not to adversely affect the mitochondrial potential. Each curve represents 10,000 events. (D) Cells were treated for 18 hours and analyzed for ATP production using the CellTiter-Glo Luminescent cell viability assay kit. MSW showed a small but significant decrease in ATP production. Bar represents standard error of the means of three samples per condition. (E and F) Untreated and treated cells were extracted with 0.05 percent Triton-X-100 for 1 minute to collect the cytosolic cytochrome C (CytC) and then the noncytosolic fraction extracted with RIPA to collect the membrane-bound cytochrome C; relative loading was detected by probing the gels for GAPDH. Graphs represent quantification of the cytochrome C normalized to GAPDH for comparison. Micrographs are representative of at least two experiments performed with different batches of primary cells.



mitochondrial membrane potential; this is shown by the left shift in the curve (Figure 3C).

To further confirm mitochondrial functionality, we determined the levels of ATP production in untreated cells and in cells that were treated with MSW smoke for 18 hours. We found that a 1:4 dilution of MSW solution resulted in a small, albeit significant, decrease in ATP production (Figure 3D) when compared to the control, again confirming that the mitochondria are not greatly affected. To further ascertain that mitochondrial function is not significantly affected, we examined the levels of cytochrome C in the mitochondrial membrane. After smoke treatment, cells were exposed to a low concentration of Triton-X-100 for a short period of time to collect the cytosolic contents to analyze for cytochrome C released from the mitochondrial membrane. The cell insoluble fraction was then further extracted to analyze for membrane-bound cytochrome C. The results show that there was a very small amount of cytochrome C present in the cytosol of treated and untreated cells, and a higher amount in the membrane fraction, as expected (Figure 3E and F). The level of cytochrome C in the cytosol was essentially the same in treated and untreated cells (Figure 3E), showing that MSW does not cause cytochrome C release from the mitochondrial membrane. Taken together these results show that although the mitochondria change morphology upon treatment with MSW, their function is not significantly affected by exposure to nonlethal levels of MSW smoke.

To test whether the ROS in MSW may be involved in the effects we observe on mitochondrial morphology when cells are treated with MSW, we treated the smoke solution with superoxide dismutase (SOD) and catalase (CAT) before applying them to the cells. SOD interacts with the oxygen radicals in the smoke to produce hydrogen peroxide that in turn is converted to water and oxygen by CAT. Cells treated with smoke solution containing SOD plus CAT and then stained with Mitotracker Red showed that in the presence of these ROS scavengers the effect of MSW smoke on mitochondrial fragmentation was essentially reversed (Figure 4).

We conclude that levels of MSW cigarette smoke found in the tissues *in vivo* do not induce the cells to undergo cell death and that the ROS in this type of smoke do not strongly inhibit ATP production. Therefore, we investigated potential effects that these doses might have on functions of "wound-like" fibroblasts that can affect wound healing.

#### **Effect of MSW on fibroblast migration**

Because we observed a change in cell shape with MSW treatment, we examined whether alterations occur in major cytoskeletal elements such as microtubules and microfilaments. Immunoblot analysis for tubulin

showed that MSW stimulates the cells to produce more tubulin (Figure 5A; for loading control see Figure 6A). Immunolabeling showed that the microtubules were more disorganized in the smoke-treated than in control cells (Figures 5B and C). In particular, the centrosome (from which the microtubules emanate) appears less well defined than in cells treated only with vehicle. For the microfilaments, using rhodamine phalloidin we measured more F-actin in the MSW-treated cells (Figure 5D) and observed that the stress fibers appeared thicker (not shown).

It is known that stress fibers associate with focal adhesion molecules to anchor cells to the substratum. To examine whether MSW-treated cells have more adhesion plaques, we measured the level of the focal adhesion plaque molecule vinculin in the cells and immunolabeled for the same molecule. Vinculin was markedly elevated in response to MSW treatment (Figure 6A) and treated cells showed many more focal adhesion plaques than control cells (Figure 6B and C).

Based on these results we postulated that MSW-treated fibroblasts would have impaired migration. To test this possibility, we used the cloning ring migration assay by plating the fibroblasts inside the cloning ring, allowing fibroblasts to adhere for 3 hours, removing the ring, and marking the edge of the ring formed by the cells. The cells were then immediately treated for 24 hours and migration was measured from the initial edge of the ring to where the cells migrated at

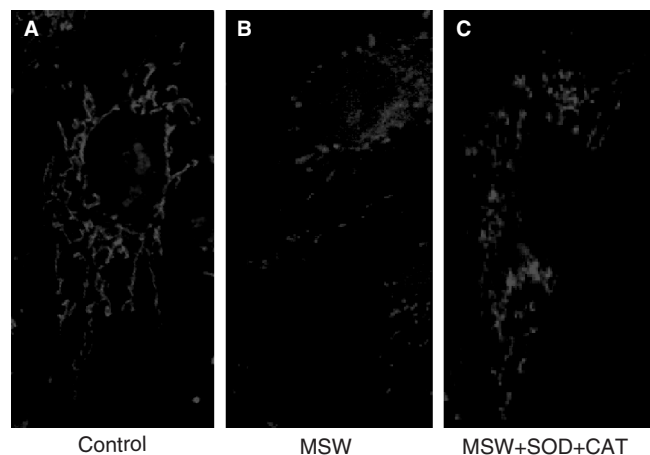


**FIGURE 4.** Effects of ROS on mitochondrial morphology in cells treated with MSW. Cells were stained with Mitotracker Red; one cell is shown for each condition. (A) Control cells; mitochondria are elongated and spread throughout the cell. (B) Cells treated with MSW; mitochondria became vesicular and more concentrated around the nucleus. (C) Cells exposed to MSW after the smoke was treated with ROS scavengers, SOD (1000 units) and CAT (500 units). These scavengers were added to the smoke solution for 10 minutes before subsequent treatment of the cells. The treatment of the smoke with the two enzymes eliminated the ability of MSW to cause change in mitochondrial morphology. Figures are representative of three experiments or more.

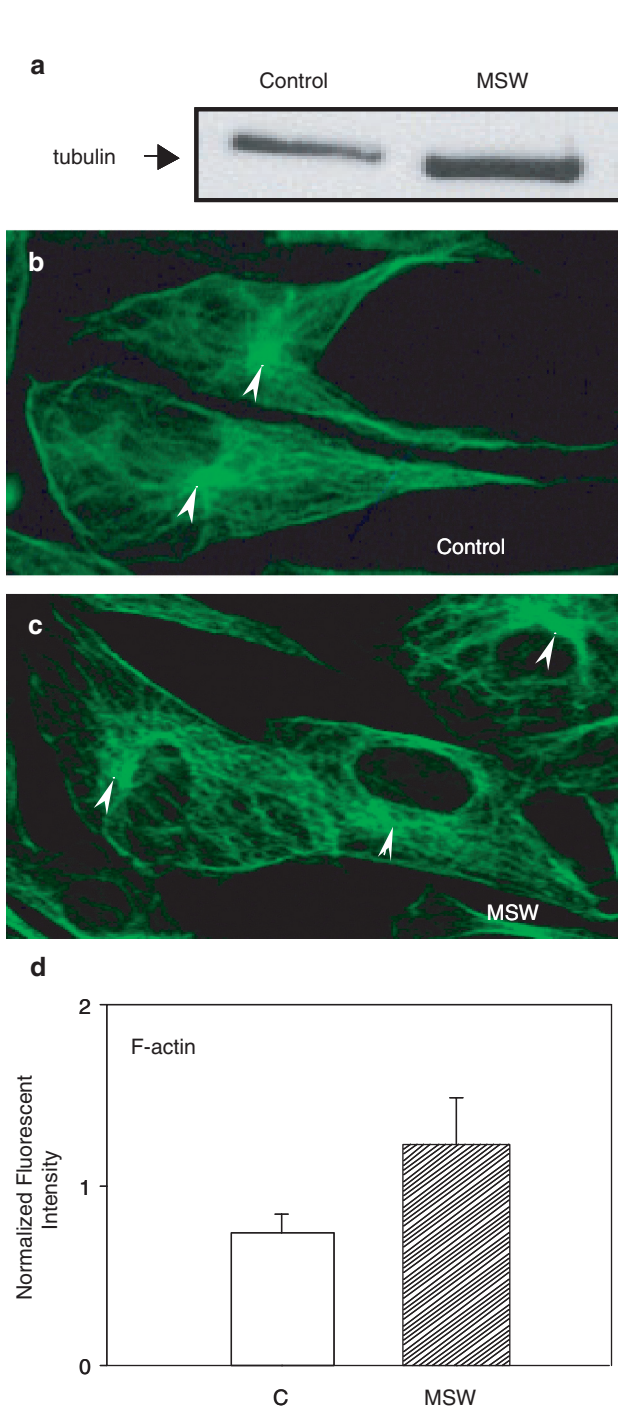


**FIGURE 5.** Effect of MSW on microtubules and microfilaments. (A) Immunoblot analysis showed an increase in tubulin after smoke treatment. (B) Microtubules in control cells showed typical bright centrosomal staining (arrowheads) with microtubules radiating outward throughout the cytosol. (C) MSW-treated cells showed a much less ordered extension of the microtubules and the centrosomes (arrowheads) were much less organized than in the control. (D) Rhodamine phalloidin was used to stain microfilaments (F-actin) and fluorescence intensity was measured at 550–580nm using a fluorimeter. MSW-treated cells contained more F-actin than the control cells. Bar represents standard error of the means of three samples per condition.

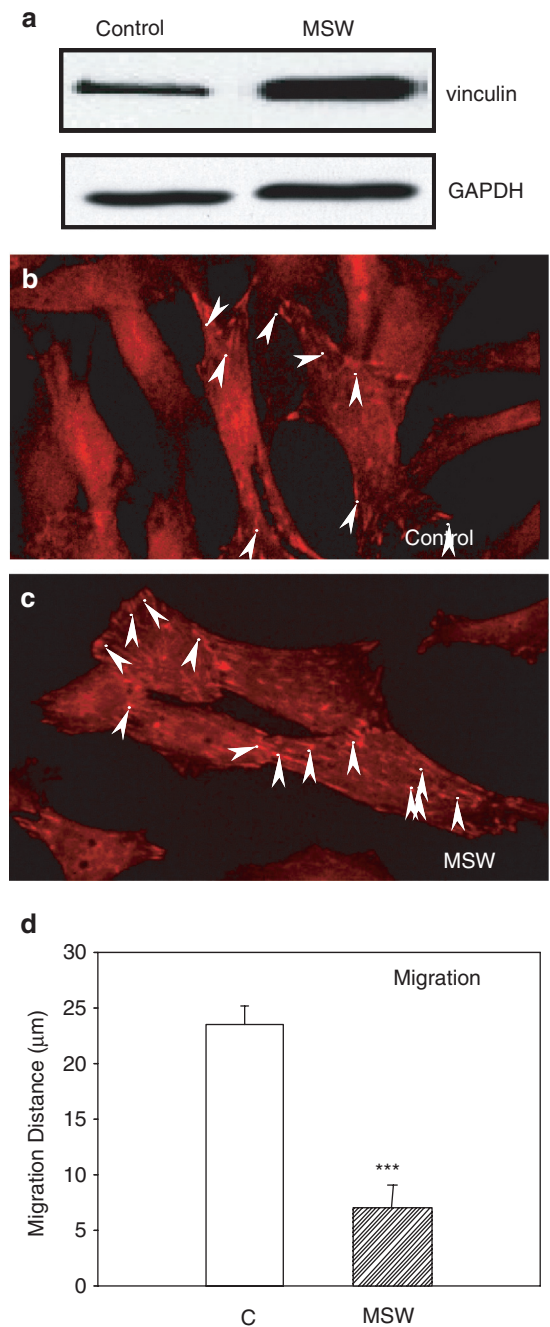


**FIGURE 6.** Effect of MSW on focal adhesion plaques and cell migration. (A) Immunoblot analysis for vinculin showed that MSW stimulates a marked increase in the level of this protein. (B and C) Immunolabeling for vinculin showed that treated fibroblasts also have many more focal adhesion plaques (arrowheads). (D) Cells were plated inside a cloning ring and allowed to adhere for 3 hours. Upon removal of the cloning ring, the boundary of the cell region was marked. The cells were then treated with MSW and permitted to migrate for 24 hours. The distance migrated by the cells was measured from the initial ring edge to the leading edge of the migrating cells. MSW strongly inhibited fibroblast migration, correlating well with the increased level of focal adhesion plaques. Figures are representative of at least three experiments performed with different batches of primary cells. Bars represent standard errors of the means of at least three samples per condition.

24 hours. We found that MSW significantly decreased the ability of the cells to migrate (Figure 6D).

### Effects of MSW on fibroblast survival

In addition to the effects described above, we also observed that the cells treated with our doses of MSW smoke appear to survive better than the control in long-term cultures. To ascertain whether cell proliferation was affected by MSW smoke, cells were treated as above and either counted or exposed to BrdU at the beginning of the experiment. Cell counts showed that smoke treatment does not affect cell number (Figure 7A), whereas BrdU incorporation showed that MSW inhibited cell division (Figure 7B). Due to the profound decrease in BrdU incorporation during the period of 18 hours, we have performed longer treatments (24 hours) in more

sensitive cells, such as human dermal fibroblasts, and shown that these cells are not lethally damaged; the level of ATP after treatment remained high (Figure 7C). Furthermore, we performed a recovery experiment where we challenged the cells for several consecutive treatments with two recoveries in between the treatments to detect whether the cells were damaged. After the final treatment, the MSW-treated cell number was similar to the control, indicating that the cells did not undergo cell death (Figure 7D). This apparently conflicting result led us to hypothesize that nonlethal concentrations of MSW stimulate fibroblasts to survive better.

To test this possibility, we treated cells with MSW for 18 hours and then replaced the treatment with complete media for 24 hours, which is sufficient to allow these cells to undergo one round of cell division. These cells were then subjected to another 18 hours of

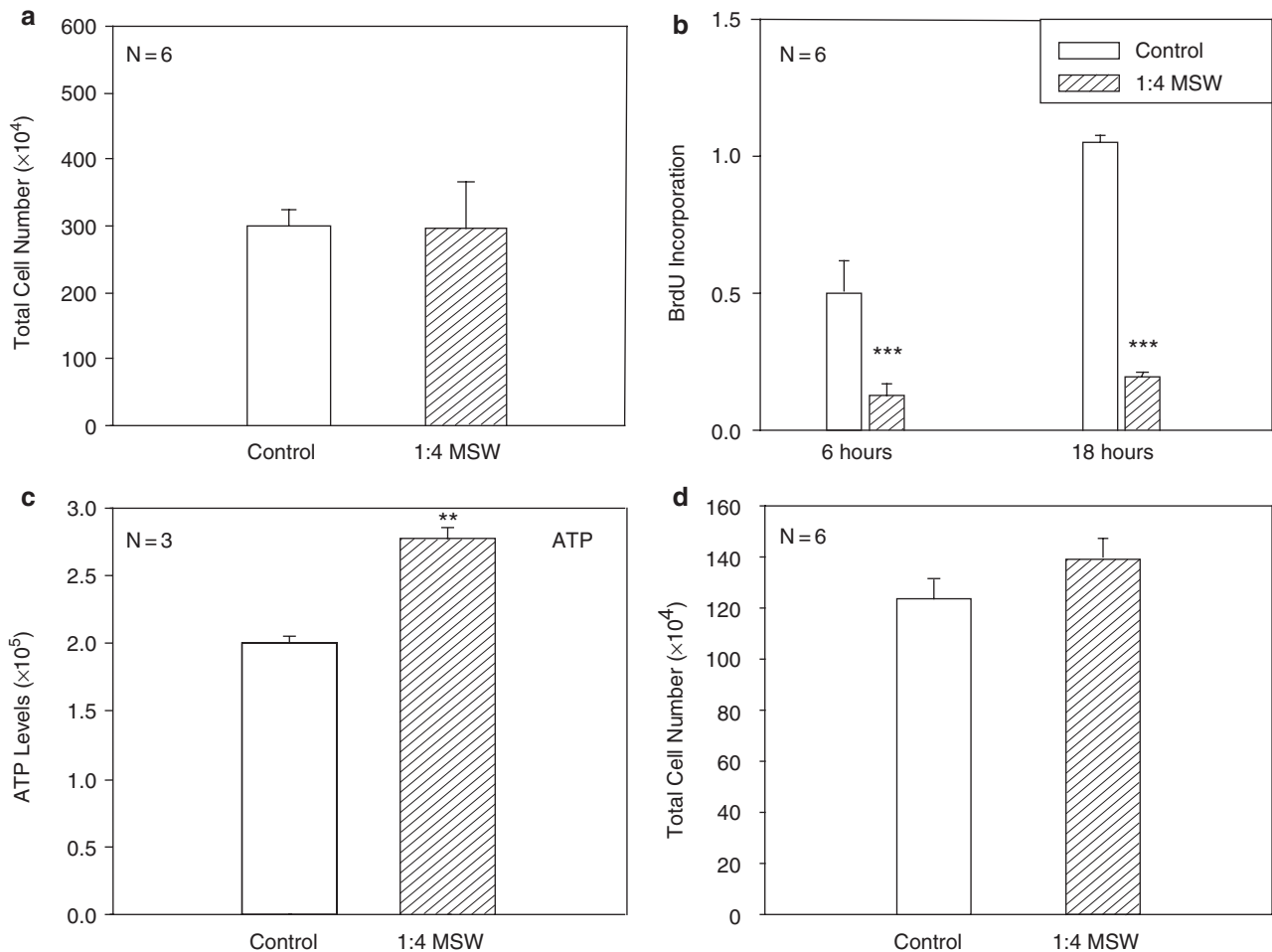


**FIGURE 7.** Effects of MSW treatment on fibroblast division. (A) Cells were treated with MSW smoke solution for 24 hours and the total cell number was counted. There was no significant difference between controls and treated cells. (B) Fibroblasts were plated in 96-well plates, allowed to grow to confluency, MSW and BrdU were added to the cultures, and the cells allowed to incorporate BrdU for the indicated time points. At both 6 and 18 hours, MSW-treated cells showed a large decrease in BrdU incorporation when compared to the control. (C) Normal human dermal fibroblasts treated for 24 hours show that the cells are not lethally damaged. (D) Cells treated for 18 hours, three times with two recovery periods (24 hours) in between each treatment. The MSW-treated cell number is similar to the control, indicating that the cells did not undergo cell death.

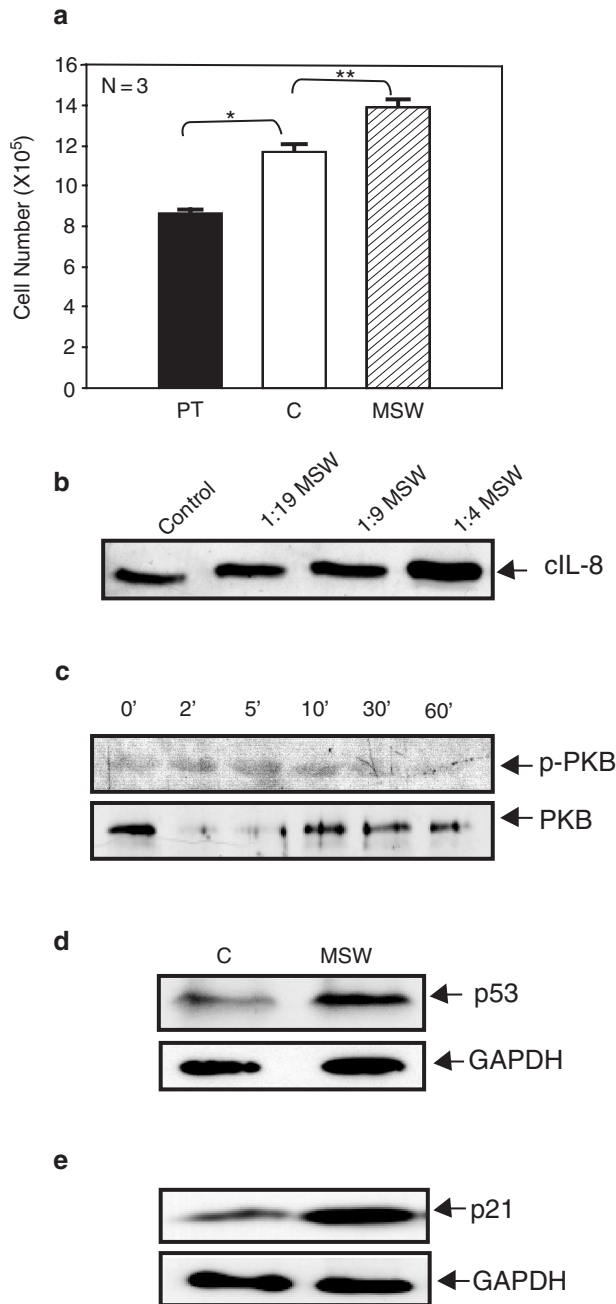


**FIGURE 8.** Effects of MSW treatment on fibroblast survival. (A) Confluent fibroblasts were treated for 18 hours, allowed to recover for 24 hours to give the opportunity for the cells to divide, and finally treated again for another 18 hours to look at the ability for cell recovery. The total cell numbers were counted. The number of cells after MSW treatment was significantly higher than in the control group. PT = cell number before treatment began (Pre-treatment). (B-E) Primary fibroblasts were treated with MSW as indicated. MSW stimulated an increase in the immediate early stress-response protein, IL-8 (B), and phosphorylated PKB/Akt (C). MSW-treated cells also showed an increased level of p53 (D) and p21 (E). GAPDH was used to indicate the levels of protein loading. Because the supernatant does not contain GAPDH, we verify equal loading of IL-8 gels by using coomassie staining of identical samples. Each figure is a representative of at least two experiments.

treatment to determine whether the cells are able to survive better upon smoke treatment (Figure 8A). We found that after treatment, the number of cells in the cultures exposed to MSW was significantly higher ( $p < 0.01$ ) than the number of cells in the controls after treatment with medium only (C) and prior to treatment (PT). These results suggest that cells not only survived well after treatment with doses of smoke similar to those found in the tissues of smokers in vivo, but survived more efficiently than the control cells. Based on these results we raised the possibility that MSW-treated cells turn on stress response proteins that then allow them to survive well the stressful environment. Therefore, we examined the expression and/or activation of proteins that are known to be involved in cell survival such as IL-8, an early stress response protein, protein kinase B (PKB/Akt, a cell survival protein), p53 and p21 (cell cycle regulatory and survival proteins).

MSW stimulated an increase in the levels of IL-8 in a dose-dependent manner (Figure 8B) and induced phosphorylation/activation of PKB/Akt in a time-dependent manner shortly after smoke exposure (Figure 8C). The level of p53, a protein critical for cell survival, was also elevated upon MSW treatment (Figure 8D). Because it is known that p53 can stimulate expression of p21, a protein that increases cell survival involving PKB/Akt,<sup>36</sup> we investigated whether MSW also increases p21 and found that it did (Figure 8E). These results support the idea that when fibroblasts are treated with nonlethal levels of MSW smoke, they respond better to the stresses imposed by the toxicants present in the smoke, and hence are able to survive better. We currently are determining the mechanisms by which these proteins lead to cell survival as a result of exposure to MSW smoke.

## DISCUSSION

Despite the common belief that smoking “moderately” is not very damaging, we show here that doses of cigarette smoke that do not kill cells can have potentially serious effects on health. Moderate doses of MSW minimally affect ATP production by primary fibroblasts, but they stimulate production/activation of stress response proteins that are known to be survival factors. As a consequence, when cells treated with these smoke levels are allowed to recover, they do not divide faster but they survive better than cells not exposed to smoke. We show that the minimal effects on ATP production are probably due to morphological rather than functional changes in the mitochondria and that ROS in the smoke play an important role in this effect. We also show that these levels of cigarette smoke cause alterations in the cytoskeleton and in cell adhesion molecules resulting in inhibition of cell

migration, a process critical for proper wound healing. These data suggest that fibroblasts exposed to nonlethal levels of "first-hand" smoke are invigorated by survival factors, increasing their life span and leading to a net accumulation of these cells. This effect may lead to a buildup of connective tissue, potentially resulting in over-healing or fibrosis of organs. In the case of open wounds, exposure to smoke could result in nonclosure of the wound for lack of proper fibroblast migration into the healing tissue.

Cells respond to insults by stimulating the expression/production of stress response proteins. Whereas this is a defense mechanism for cell survival, constant stimulation may lead not only to short-term survival responses but also to a more sustained stimulation of these proteins. Therefore, increased production/activation of these proteins has implications for diseases such as cancer and fibrosis. In particular, MSW stimulates an increase in the levels of p53 and p21. These two proteins have been implicated in cell survival by initiating processes that allow the cells to repair their DNA.<sup>36-38</sup> In general, p53, when activated, binds to the promoter region of p21 and induces p21 expression, leading to DNA repair during cell cycle arrest.

Our results show that ROS are involved in the observed effect of MSW on mitochondrial morphology. The mechanism of the specific effect on the mitochondria by MSW is unclear at this point. It is known that dynamin-related GTPase Dnm1p, Net2p, Mdv1p, Fis1p, and Fzo1<sup>39-42</sup> are involved in mitochondrial fission/fusion in yeast. In mammalian cells, however, these mitochondrial processes are less well understood. The most well studied mammalian homolog implicated in mitochondrial fission is the dynamin-like protein 1 and it has been shown to be involved in causing aberrant mitochondrial morphology (i.e., punctuated mitochondria) under environmental stress.<sup>43-45</sup> Thus, we speculate that this protein could be involved in causing the vesicular morphology we observed in our studies. We are currently investigating this possibility.

Our observations that MSW disrupts microtubule patterns in fibroblasts may have important implications for impaired wound healing. In MSW-treated fibroblasts, the microtubules are not as well organized as in control cells. Microtubules are major cytoskeletal elements that help carry signaling molecules and organelles to different parts of the cell so they can perform their tasks efficiently. Therefore, the effects of MSW on microtubule organization may also have implications for the effects we observe on the mitochondria. Mitochondria are not randomly distributed in cells but are organized along microtubules, hence changes in the structure of the microtubule may very well affect the distribution and shape of these organelles.<sup>46</sup> Disruption of the microtubules could contribute to mitochondrial fragmentation and accumulation in the perinuclear

region.<sup>46</sup> Given that the slightly reduced levels of ATP are not due to a loss of the mitochondrial membrane potential, it is possible that this decrease in ATP production is a result of the mitochondrial morphological changes we observed. This is consistent with findings showing that the aqueous phase of cigarette smoke caused mitochondrial swelling but did not disrupt the inner mitochondrial membrane.<sup>47</sup> The disruption of the microtubule organizing center or centrosome may also have implications for cell motility (see below). For example, CDC42, a GTPase that is involved in cell migration is also involved in orientation of the microtubule organizing center. Similarly, the Rho GTPase bridges communication between microtubules and microfilaments, cytoskeletal elements that are involved in cell motility.

We also demonstrated an increase in focal plaques and their adhesion molecules, such as vinculin and F-actin that most likely contribute to the decrease in cell migration we observe. These results further suggest a potential mechanism by which smokers have impaired wound healing; an increase in focal adhesions and microfilaments would potentially lead to a loss of fibroblast migration into the wound site. A major characteristic of wound fibroblasts during wound repair is migration into the wound site to secrete growth factors and cytokines and to deposit and remodel the ECM. If these processes are disrupted, the wound will heal poorly, potentially resulting in open sores. In smokers, this is a very common problem such that they are often advised by surgeons to stop smoking for a period of time before undergoing surgery.<sup>7,8,48,49</sup> In conclusion, we have shown that nonlethal levels of firsthand smoke, in spite of being rich in ROS, do not significantly affect mitochondrial function nor do they stimulate cell death. However, these levels of smoke stimulate proteins that increase cell survival and inhibit cell migration. These findings suggest that nonlethal levels of smoke may cause significant damage to the healing process. Indeed, an increase in fibroblast survival may lead to fibrosis whereas a decrease in fibroblast migration may lead to abnormal wound closure, both of which are found to occur in smokers. Furthermore, in situations in which DNA mutations occur and cells become malignant, an increase in cell survival would greatly enhance the ability of tumors to survive.

## ACKNOWLEDGMENTS

We thank E. Nothnagel and Madhav Yadhav for helping us with quantitation of the smoke solution. We thank the P. Talbot laboratory for the use of the smoking machine, Barbara Walter in L. Owen's laboratory for help with the FACS analysis, F. Sladek for the use of the luminometer, A. Grosovsky for the use of the

coulter counter, and X. Liu for the p53 antibody. We also thank Qi-Jing Li for his help with the confocal pictures and the other colleagues in the laboratory for helpful discussion. Part of this work was performed in the University of California at Riverside Confocal Microscope Facility. This work was partially supported by AHA grant #0050732Y, TRDRP grant# 10IT-0170 and 11DT-0244.

## REFERENCES

1. Rees TD, Liverett DM, Guy CL. The effect of cigarette smoking on skin-flap survival in the face lift patient. *Plast Reconstr Surg* 1984;73:911-5.
2. Riefkohl R, Wolfe JA, Cox EB, McCarty KS Jr. Association between cutaneous occlusive vascular disease, cigarette smoking, and skin slough after rhytidectomy. *Plast Reconstr Surg* 1986;77:592-5.
3. Kroll SS. Necrosis of abdominoplasty and other secondary flaps after TRAM flap breast reconstruction. *Plast Reconstr Surg* 1994;94:637-43.
4. Bailey MH, Smith JW, Casas L, Johnson P, Serra E, de la Fuente R, Sullivan M, Scanlon EF. Immediate breast reconstruction: reducing the risks. *Plast Reconstr Surg* 1989;83:845-51.
5. Hartrampf CR Jr, Bennett GK. Autogenous tissue reconstruction in the mastectomy patient. A critical review of 300 patients. *Ann Surg* 1987;205:508-19.
6. Krueger JK, Rohrich RJ. Clearing the smoke: the scientific rationale for tobacco abstinence with plastic surgery. *Plast Reconstr Surg* 2001;108:1063-73; discussion 1074-7.
7. Netscher DT, Clamon J. Smoking: adverse effects on outcomes for plastic surgical patients. *Plast Surg Nurs* 1994;14:205-10.
8. Nolan J, Jenkins RA, Kurihara K, Schultz RC. The acute effects of cigarette smoke exposure on experimental skin flaps. *Plast Reconstr Surg* 1985;75:544-51.
9. Czernin J, Waldherr C. Cigarette smoking and coronary blood flow. *Prog Cardiovasc Dis* 2003;45:395-404.
10. Boyd AS, Stasko T, King LEJ, Cameron GS, Pearse AD, Gaskell SA. Cigarette smoke produces airway wall remodeling in rat tracheal explants. *J Am Acad Dermatol* 1999;41:23-6.
11. Frances C, Boisnic S, Hartmann DJ, Dautzenberg B, Branchet MC, Charpentier YL, Robert L. Changes in the elastic tissue of the non-sun-exposed skin of cigarette smokers. *Br J Dermatol* 1991;125:43-7.
12. Akoz T, Akan M, Yildirim S. If you continue to smoke, we may have a problem: smoking's effects on plastic surgery. *Aesth Plast Surg* 2002;26:477-82.
13. Otto GH, Buyukcakar C, Fife CE. Effects of smoking on cost and duration of hyperbaric oxygen therapy for diabetic patients with non-healing wounds. *Undersea Hyperb Med* 2000;27:83-9.
14. Sorensen LT, Horby J, Friis E, Pilsgaard B, Jorgensen T. Smoking as a risk factor for wound healing and infection in breast cancer surgery. *Eur J Surg Oncol* 2002;28:815-20.
15. Siana JE, Rex S, Gottrup F. The effect of cigarette smoking on wound healing. *Scand J Plast Reconstr Surg Hand Surg* 1989;23:207-9.
16. Clark R, editor. *The molecular and cellular biology of wound repair*. New York: Plenum Press, 1996.
17. Gabbiani G. The myofibroblast in wound healing and fibrocontractive diseases. *J Pathol* 2003;200:500-3.
18. Pryor WA. Cigarette smoke radicals and the role of free radicals in chemical carcinogenicity. *Environ Health Perspect* 1997;105 (Suppl. 4):875-82.
19. Comhair SA, Erzurum SC. Antioxidant responses to oxidant-mediated lung diseases. *Am J Physiol Lung Cell Mol Physiol* 2002;283:L246-55.
20. Knoll M, Talbot P. Cigarette smoke inhibits oocyte cumulus complex pick-up by the oviduct in vitro independent of ciliary beat frequency. *Reprod Toxicol* 1998;12:57-68.
21. Li QJ, Vaingankar S, Sladek FM, Martins-Green M. Novel nuclear target for thrombin: activation of the Elk1 transcription factor leads to chemokine gene expression. *Blood* 2000;96:3696-706.
22. Vaingankar SM, Martins-Green M. Thrombin activation of the 9E3/CEF4 chemokine involves tyrosine kinases including c-src and the epidermal growth factor receptor. *J Biol Chem* 1998;273:5226-34.
23. Feugate JE, Li Q, Wong L, Martins-Green M. The cxc chemokine cCAF stimulates differentiation of fibroblasts into myofibroblasts and accelerates wound closure. *J Cell Biol* 2002;156:161-72.
24. Feugate J, Wong L, Li QJ, Martins-Green M. The CXC chemokine cCAF stimulates precocious deposition of ECM molecules by wound fibroblasts, accelerating development of granulation tissue. *BMC Cell Biol* 2002;3:13.
25. Brown LF, Dubin D, Lavigne L, Logan B, Dvorak HF, Van de Water L. Macrophages and fibroblasts express embryonic fibronectins during cutaneous wound healing. *Am J Pathol* 1993;142:793-801.
26. Environmental Protection Agency. EPA Report/600/6-90/006F: Respiratory health effects of passive smoking: lung cancer and other disorders. Washington, DC, 1992.
27. Al-Delaimy WK, Mahoney GN, Speizer FE, Willett WC. Toenail nicotine levels as a biomarker of tobacco smoke exposure. *Cancer Epidemiol Biomarkers Prev* 2002;11:1400-4.
28. Wolff D, Wathanapongsiri A, Vedral D. Nicotine in blood in relation to smoking. *J Pharmacol Exp Therap* 1949;95:145-8.
29. Armitage AK, Dollery CT, George CF, Houseman TH, Lewis PJ, Turner DM. Absorption and metabolism of nicotine from cigarettes. *Br Med J* 1975;4:313-6.
30. Russell MA, Jarvis M, Iyer R, Feyerabend C. Relation of nicotine yield of cigarettes to blood nicotine concentrations in smokers. *Br Med J* 1980;280:972-6.
31. Kogan MJ, Verebey K, Jaffee JH, Mule SJ. Simultaneous determination of nicotine and cotinine in human plasma by nitrogen detection gas-liquid chromatography. *J Forensic Sci* 1981;26:6-11.
32. Schwartz SL, Gastonguay MR, Robinson DE, Balter NJ. Physiologically based pharmacokinetic modeling of nicotine. In: Gorrod JW, Wahren J, editors. *Nicotine and related alkaloids: absorption, distribution, metabolism and excretion*. New York: Chapman & Hall, 1993:255-74.
33. Kyerematen GA, Vesell ES. Metabolism of nicotine. *Drug Metab Rev* 1991;23:3-41.
34. Tsujimoto A, Nakashima T, Tanino S, Dohi T, Kurogochi Y. Tissue distribution of [<sup>3</sup>H]nicotine in dogs and rhesus monkeys. *Toxicol Appl Pharmacol* 1975;32:21-31.
35. Plowchalk DR, Andersen ME, deBethizy JD. A physiologically based pharmacokinetic model for nicotine disposition in the Sprague-Dawley rat. *Toxicol Appl Pharmacol* 1992;116:177-88.
36. Li Y, Dowbenko D, Lasky LA. AKT/PKB phosphorylation of p21Cip/WAF1 enhances protein stability of p21Cip/WAF1 and promotes cell survival. *J Biol Chem* 2002;277:11352-61.
37. Helt CE, Rancourt RC, Stavarsky RJ, O'Reilly MA. p53-dependent induction of p21 (Cip1/WAF1/Sdi1) protects against oxygen-induced toxicity. *Toxicol Sci* 2001;63:214-22.
38. Whyte DA, Broton CE, Shillitoe EJ. The unexplained survival of cells in oral cancer: what is the role of p53? *J Oral Pathol Med* 2002;31:125-33.
39. Yoon Y, McNiven MA. Mitochondrial division: new partners in membrane pinching. *Curr Biol* 2001;11:R67-70.
40. Wong ED, Gorsich SW, McCaffery JM, Shaw JM, Nunnari J. The dynamin-related GTPase, Mgm1p, is an

- intermembrane space protein required for maintenance of fusion competent mitochondria. *J Cell Biol* 2000;151:341–52.
41. Cervený KL, McCaffery JM, Jensen RE. Division of mitochondria requires a novel DMN1-interacting protein, Net2p. *Mol Biol Cell* 2001;12:309–21.
  42. Catlett NL, Weisman LS. Divide and multiply: organelle partitioning in yeast. *Curr Opin Cell Biol* 2000;12:509–16.
  43. Smirnova E, Shurland DL, Ryazantsev SN, van der Bliek AM. A human dynamin-related protein controls the distribution of mitochondria. *J Cell Biol* 1998;143:351–8.
  44. Pitts KR, Yoon Y, Krueger EW, McNiven MA. The dynamin-like protein DLP1 is essential for normal distribution and morphology of the endoplasmic reticulum and mitochondria in mammalian cells. *Mol Biol Cell* 1999;10:4403–17.
  45. Frank S, Gaume B, Bergmann-Leitner ES, Leitner WW, Robert EG, Catez F, Smith CL, Youle RJ. The role of dynamin-related protein 1, a mediator of mitochondrial fission, in apoptosis. *Dev Cell* 2001;1:515–25.
  46. Hollenbeck PJ. The pattern and mechanism of mitochondrial transport in axons. *Front Biosci* 1996;1:d91–d102.
  47. Gairola C, Aleem MI. Cigarette smoke: effect of aqueous and nonaqueous fractions on mitochondrial function. *Nature* 1973;241:287–8.
  48. Mosely LH, Finseth F. Cigarette smoking: impairment of digital blood flow and wound healing in the hand. *Hand* 1977;9:97–101.
  49. Mosely LH, Finseth F, Goody M. Nicotine and its effect on wound healing. *Plast Reconstr Surg* 1978;61:570–5.